BJP British Journal of Pharmacology

DOI:10.1111/bph.12302
www.brjpharmacol.org

RESEARCH PAPER

Emodin inhibits growth and induces apoptosis in an orthotopic hepatocellular carcinoma model by blocking activation of STAT3

Aruljothi Subramaniam[1,2]*, Muthu K Shanmugam[1]*, Tina H Ong[3], Feng Li[1], Ekambaram Perumal[2], Luxi Chen[4,5], Shireen Vali[6], Taher Abbasi[6], Shweta Kapoor[7], Kwang Seok Ahn[8], Alan Prem Kumar[1,5,9,10], Kam M Hui[3] and Gautam Sethi[1,5]

[1]*Department of Pharmacology, Yong Loo Lin School of Medicine, National University of Singapore, Singapore,* [2]*Molecular Toxicology Lab, Department of Biotechnology, Bharathiar University, Coimbatore, India,* [3]*Division of Cellular and Molecular Research, Humphrey Oei Institute of Cancer Research, National Cancer Centre, Singapore,* [4]*Department of Biochemistry, Yong Loo Lin School of Medicine, National University of Singapore, Singapore,* [5]*Cancer Science Institute of Singapore, Centre for Translational Medicine, Singapore,* [6]*Cellworks Group Inc., Saratoga, CA, USA,* [7]*Cellworks Research India Pvt. Ltd, Bangalore, India,* [8]*College of Oriental Medicine, Kyung Hee University, Seoul, Korea,* [9]*School of Biomedical Sciences, Faculty of Health Sciences, Curtin University, Perth, WA, Australia, and* [10]*Department of Biological Sciences, University of North Texas, Denton, TX, USA*

Correspondence
Dr Gautam Sethi, Department of Pharmacology, Yong Loo Lin School of Medicine, National University of Singapore, Singapore 117597. E-mail: phcgs@nus.edu.sg;
Professor Kam M Hui, Division of Cellular and Molecular Research, Humphrey Oei Institute of Cancer Research, National Cancer Centre, Singapore 169610. E-mail: cmrhkm@nccs.com.sg

*AS and MKS contributed equally to this work.

Keywords
STAT3; emodin; hepatocellular carcinoma; apoptosis; proliferation

Received
2 November 2012
Revised
4 July 2013
Accepted
8 July 2013

BACKGROUND AND PURPOSE

Aberrant activation of STAT3 is frequently encountered and promotes proliferation, survival, metastasis and angiogenesis in hepatocellular carcinoma (HCC). Here, we have investigated whether emodin mediates its effect through interference with the STAT3 activation pathway in HCC.

EXPERIMENTAL APPROACH

The effect of emodin on STAT3 activation, associated protein kinases and apoptosis was investigated using various HCC cell lines. Additionally, we also used a predictive tumour technology to analyse the effects of emodin . The *in vivo* effects of emodin were assessed in an orthotopic mouse model of HCC.

KEY RESULTS

Emodin suppressed STAT3 activation in a dose- and time-dependent manner in HCC cells, mediated by the modulation of activation of upstream kinases c-Src, JAK1 and JAK2. Vanadate treatment reversed emodin-induced down-regulation of STAT3, suggesting the involvement of a tyrosine phosphatase and emodin induced the expression of the tyrosine phosphatase SHP-1 that correlated with the down-regulation of constitutive STAT3 activation. Interestingly, silencing of the SHP-1 gene by siRNA abolished the ability of emodin to inhibit STAT3 activation. Finally, when administered i.p., emodin inhibited the growth of human HCC orthotopic tumours in male athymic nu/nu mice and STAT3 activation in tumour tissues.

CONCLUSIONS AND IMPLICATIONS

Emodin mediated its effects predominantly through inhibition of the STAT3 signalling cascade and thus has a particular potential for the treatment of cancers expressing constitutively activated STAT3.

Abbreviations

HCC, hepatocellular carcinoma; MTT, 3-(4,5-dimethylthiazol-2-yl)-2, 5-diphenyl-2H-tetrazolium bromide

© 2013 The British Pharmacological Society

Introduction

Hepatocellular carcinoma (HCC) is one of the most common malignancies of the liver and the fourth leading cause of cancer-related deaths worldwide (Ferlay *et al.*, 2010). The disease is more commonly encountered in rapidly developing countries such as China and major risk factors include chronic infections with hepatitis B and C viruses, alcohol abuse and exposure to food contaminants such as aflatoxin B (Lin *et al.*, 2011; Subramaniam *et al.*, 2013b). Current treatment options, including surgical resection and conventional chemotherapy, are commonly associated with severe morbidity, side effects, and also limited by the development of drug resistance (Cervello *et al.*, 2012; Subramaniam *et al.*, 2013b). Hence, novel agents that are non-toxic and efficacious are urgently needed for the prevention and treatment of HCC.

STAT proteins were originally discovered as latent cytoplasmic transcription factors almost two decades ago (Ihle, 1996). Among the different STATs, one STAT member, STAT3, is often constitutively active in various human cancers, including HCC, breast cancer, prostate cancer, head and neck squamous cell carcinoma, multiple myeloma and several other malignancies, and controls the expression of multiple genes involved in initiation, progression and chemoresistance (Wang *et al.*, 2011). Once activated, STAT3 undergoes phosphorylation-induced homodimerization, leading to nuclear translocation, DNA binding and subsequent gene transcription. STAT3 has been reported to modulate the expression of genes involved in anti-apoptosis, such as (Bcl-xl, Bcl-2 and survivin), proliferation (cyclin D1) and angiogenesis (VEGF) (Grivennikov and Karin, 2010). STAT3 is considered as an important target for HCC therapy because blockade of STAT3 has been found to induce growth arrest and apoptosis of HCC cells by various investigators (Subramaniam *et al.*, 2013b).

One major source of pharmacological inhibitors of the STAT3 system is that derived from natural sources, as around 70% of all anti-cancer drugs being used in clinical therapy are isolated from natural sources or bear a close structural relationship to compounds of natural origin (Newman, 2008). Our research group is actively exploring the potential application of natural compounds as STAT3 inhibitors in various cancer models, including HCC, and has identified several potent compounds with anti-HCC activity (Subramaniam *et al.*, 2013b). In the present study, we describe a compound called emodin (1,3,8-trihydroxy-6-methylanthraquinone), isolated from the rhizome of *Rheum palmatum* L. that has been previously reported to exhibit antiviral, anti-inflammatory, anti-ulcerogenic, immunosuppressive, pro-apoptotic and chemopreventive activities (Xia *et al.*, 2009; Tabolacci *et al.*, 2010), primarily mediated through the activation of caspase-3 (Chen *et al.*, 2002) and up-regulation of p53 and p21 (Shieh *et al.*, 2004). Moreover, emodin has been reported to enhance TNF-related apoptosis-inducing ligand-induced apoptosis (Subramaniam *et al.*, 2013a); inhibit the kinase activity of p56lck, HER2/neu (Wang *et al.*, 2001) and casein kinase (Battistutta *et al.*, 2000); suppress activation of NF-κB/AP-1 (Huang *et al.*, 2004), Akt (Brown *et al.*, 2007) and p38/Erk MAP kinases (Wang *et al.*, 2007); and block the expression of the chemokine receptor CXCR4 (Manu *et al.*, 2013; receptor nomenclature follows Alexander *et al.*, 2011). These reports suggest that emodin may be a suitable candidate agent for cancer treatment, although the detailed mechanism(s) of its action have not been completely elucidated so far.

Because of the critical role of STAT3 in tumour cell survival, proliferation and angiogenesis, and its aberrant expression in HCC, we investigated whether emodin could mediate its anti-cancer effects in part through the modulation of the STAT3 activation pathway. Alongside testing the effects of emodin in HCC cell lines and mouse model, we also investigated the involvement of the inhibition of STAT3 in the mechanism of action of emodin, using a virtual predictive tumour cell system (Rajendran *et al.*, 2011). Thus, using a novel approach of combination of predictive virtual hypothesis testing along with experimental validations, we found that emodin can indeed suppress the deregulated activation of STAT3 in HCC cells. This suppression decreased cell survival and down-regulated expression of various proliferative, anti-apoptotic and angiogenic gene products, leading to inhibition of proliferation, and induction of apoptosis in HCC cells. Emodin also significantly suppressed the growth of human HCC cells in an orthotopic mouse model and modulated the activation of STAT3 in tumour tissues.

Methods

Cell lines

The human HCC cell lines HepG2, PLC/PRF/5, Hep3B and C3A cells were obtained from American Type Culture Collection (Manassass, VA, USA). All the HCC cells were cultured in DMEM containing 1X antibiotic-antimycotic solution with 10% FBS. HepG2 cell lines were used to study the effect of emodin on constitutive STAT3 signalling cascade because they express constitutively active STAT3; HUH-7 cells were used to study the effect of emodin on inducible STAT3 signalling; PLC/PRF/5 cells were used for transfection experiments because they are relatively easy to transfect; and C3A cells were used for proliferation assays to investigate whether emodin can modulate proliferation of wide variety of HCC cells. The HCCLM3 cell line used for the *in vivo* experiments was a kind gift of Professor Zhao-You Tang at the Liver Cancer Institute (Zhongshan Hospital, Fudan University, Shanghai). HCCLM3 cells were cultured in high glucose DMEM containing 1X antibiotic-antimycotic solution with 10% FBS. The human multiple myeloma cell line U266 was kindly provided by Dr Chng Wee Joo at National University Hospital, Singapore, and human breast cancer MDA-MB-231 cells were obtained from American Type Culture Collection. These cells were cultured in RPMI 1640 medium containing 1x antibiotic-antimycotic with 10% FBS.

Western blotting

Western blot analysis was performed using a method described previously (Rajendran *et al.*, 2011).

Immunocytochemistry for STAT3 localization

Immunocytochemistry assay was performed as described previously (Rajendran *et al.*, 2011).

STAT3 luciferase reporter assay

Immunocytochemistry assay was performed as described previously (Rajendran *et al.*, 2011).

DNA binding assay

DNA binding assay was performed as described previously (Rajendran *et al.*, 2012).

Predictive experiments on virtual tumour cells

Predictive experiments were performed using the human physiologically aligned and extensively validated Virtual Tumor Cell technology (Cellworks Group Inc, Saratoga, CA, USA) (Roy *et al.*, 2010). The Cellworks tumour cell platform provides a dynamic and transparent view of tumour cell physiology at the functional proteomics abstraction level. The platform's open-access architecture provides a framework for different 'what-if' experiments and analysis in an automated high-throughput methodology.

Platform description

The virtual tumour cell platform consists of a dynamic and kinetic representation of the signalling pathways underlying tumour physiology at the bio-molecular level with coverage on all the key tumour phenotypes including proliferation, viability, angiogenesis, metastasis, apoptosis, tumour metabolism and tumour microenvironment related to associated inflammation. The technology is a comprehensive coverage of protein players, associated gene and mRNA species with regard to tumour-related signalling. The integrated cancer system models 6516 crosstalk of around 4680 intracellular biological objects that interact via 25 180 kinetic parameters. This comprises a comprehensive and extensive coverage of the kinome, transcriptome, proteome and, to some extent, metabolomic components. The platform includes representation of comprehensive signalling pathways such as growth factors like EGFR, PDGFRA, FGFR, c-MET, VEGFR and IGF-1R, cell cycle regulators, mTOR signalling, p53 signalling cascade, HIF signalling, apoptotic machinery, DNA damage repair, cytokine pathways such as IL1, IL4, IL6, IL12, TNF; lipid mediators and tumour metabolism and others (Rajendran *et al.*, 2011).

Predictive study experimental protocol

The virtual tumour cell was simulated in the proprietary Cellworks computational backplane and initialized to a control state wherein all bio-molecules attain control steady-state values which is aligned to normal epithelial cell physiology that is non-tumourigenic. This non-transformed epithelial cell was then triggered to align to the HCC cell line HepG2 having KRAS mutation, CDKN2A deletion and mutation in the p53 gene.

Simulation protocol

Emodin was tested on the above baseline and the biomarker trends evaluated as percentage changes from cell baseline values. Emodin was shown as an inhibitor of casein kinase 2 (CK2) along with secondary targets including PI3K, HER-family receptor 2 (Her2), VEGF receptor 2 (KDR) and induction of reactive oxygen species (ROS). The activity of CK2 was inhibited by 80% along with 50% inhibition in the activity for PI3K. Her2 and KDR were also inhibited by 50% at the activity level. The formation of H_2O_2 was also increased by 2.5-fold in the system as a part of the same protocol. To compare the effects of emodin treatment with STAT3 inhibition alone, experiments were also carried out for inhibition of STAT3 activity by 40% on HepG2 cell line.

Transfection with SHP-1 siRNA

HepG2 cells were plated in each well of six-well plates and allowed to adhere for 24 h. On the day of transfection, 4 μL of Lipofectamine (Invitrogen) was added to 50 nM SHP-1 siRNA in a final volume of 100 μL of culture medium. After 48 h of transfection, cells were treated with emodin, and whole cell extracts were prepared to investigate SHP-1, phospho-STAT3 and STAT3 expression by Western blot analysis.

MTT assay

The anti-proliferative effect of emodin against HCC cells was determined by the MTT dye uptake method as described previously (Rajendran *et al.*, 2011).

Real-time PCR

Real-time PCR assay for Bcl-2, Bcl-xl, cyclin D1, VEGF and Mcl-1 was performed as described previously (Rajendran *et al.*, 2012).

Live/dead assay

Apoptosis of cells was also determined by live/dead assay (Molecular Probes, Eugene, OR, USA) that measures intracellular esterase activity and plasma membrane integrity as described previously (Rajendran *et al.*, 2012).

STAT3 siRNA transfection

HepG2 cells were plated in 96-well plates and allowed to adhere for 24 h. On the day of transfection, Lipofectamine was added to 50 nM control or STAT3 siRNA in a final volume of 200 μL of culture medium. After 48 h, cells were treated with indicated concentrations of emodin for 72 h and then subjected to MTT assay.

Orthotopic HCC model

All animal care and experimental procedures were reviewed and approved by Sing Health Institutional Animal Care and Use Committee. All studies involving animals are reported in accordance with the ARRIVE guidelines for reporting experiments involving animals (Kilkenny *et al.*, 2010; McGrath *et al.*, 2010). A total of 28 animals were used in the experiments described here. Eight-week-old athymic nu/nu female mice (Animal Resource Centre, Australia) were implanted orthotopically with approximately 1 mm^3 of human HCCLM3_Luc2 tumour stably expressing firefly luciferase. Tumour growth was monitored by IVIS 200 Bioluminescence Imaging System (Xenogen Corp., Alameda, CA, USA). Once increasing bioluminescence tumour signals were detected in the mice liver, mice were randomly assigned to the following three treatment groups: one group (n = 9) received five i.p. injections of 200 μL vehicle [10% DMSO, 70% cremophor/ethanol (3:1) and 20% PBS], a second group,

25 mg·kg^{-1} emodin (n = 10) and the third, 50 mg·kg^{-1} emodin (n = 9) every week for 3 weeks. Animals were killed at day 28 after first therapeutic dose injection and the tumour was harvested for subsequent analysis. For imaging, mice were given i.p. injections of 150 mg·kg^{-1} D-luciferin (Xenogen) 10 min before imaging. To quantitate tumour burden, bioluminescence signals were calculated from the imaging data using the Living Image software 3.2 (Xenogen) according to the manufacturer's protocol.

Immunohistochemical analysis of tumour samples

Solid tumours from control and emodin-treated mice were fixed with 10% phosphate buffered formalin, processed and embedded in paraffin. Sections were cut and deparafinized in xylene, and dehydrated in graded alcohol and finally hydrated in water. Antigen retrieval was performed by boiling the slide in 10 mM sodium citrate (pH 6.0) for 30 min. Immunohistochemistry was performed following the manufacturer instructions (LSAB kit; Dako, Carpinteria, CA, USA). Briefly, endogenous peroxidases were quenched with 3% hydrogen peroxide. Non-specific binding was blocked by incubation in the blocking reagent in the LSAB kit (Dako) according to the manufacturer's instructions. Sections were incubated overnight with primary antibodies as follows: anti-phospho-STAT3, CD31 and anti-caspase-3 (each at 1:100 dilution). Slides were subsequently washed several times in Tris-buffered saline with 0.1% Tween 20 and were incubated with biotinylated linker for 30 min, followed by incubation with streptavidin conjugate provided in LSAB kit (Dako) according to the manufacturer's instructions. Immunoreactive species were detected using 3,3-diaminobenzidine tetrahydrochloride as a substrate. Sections were counterstained with Gill's haematoxylin and mounted under glass coverslips. Images were taken using an Olympus BX51 microscope (magnification, 40×; Tokyo, Japan).

Data analysis

Data are expressed as the mean ± SEM. In all figures, vertical error bars denote the SEM. The significance of differences between groups was evaluated by Student's t-test or one-way ANOVA test. A P-value of less than 0.05 was considered statistically significant.

Materials

A 50 mM solution of emodin (from Aldrich, St. Louis, MO, USA), with purity of 99%, was prepared in DMSO, stored as small aliquots at –20°C, and then diluted further in cell culture medium as needed. DMSO (0.1%) was used as vehicle control for all the *in vitro* experiments. Hoechst 33342, MTT, Tris, glycine, NaCl, SDS, EGF, BSA, doxorubicin and paclitaxel were purchased from Sigma-Aldrich (St. Louis, MO, USA). RPMI 1640, FBS, 0.4% Trypan blue vital stain and antibiotic-antimycotic mixture were obtained from Invitrogen (Carlsbad, CA, USA). Rabbit polyclonal antibodies to STAT3 and mouse monoclonal antibodies against phospho-STAT3 (Tyr 705) and phospho-Akt, Akt, Bcl-2, Bcl-xL, cyclin D1, survivin, Mcl-1, SHP-1, VEGF, caspase-3, cleaved caspase-3 and PARP were obtained from Santa Cruz Biotechnology (Santa Cruz, CA, USA). Antibodies to phospho-specific Src (Tyr 416), Src, phospho-specific JAK1 (Tyr 1022/1023), JAK1, phospho-specific JAK2 (Tyr 1007/1008), JAK2 and CD31 antibodies were purchased from Cell Signalling Technology (Beverly, MA, USA). The small interfering RNA (siRNA) for SHP-1 (sc-29478) and scrambled control (sc-37007) was obtained from Santa Cruz Biotechnology. SHP-1 siRNA is a pool of three sequences: sense strand (A): CUGGUGGAGCAUUUCAAG ATT, (B): CGCAGUACAAGUUCAUCUATT and (C): CAAC CCUUCUCCUCUUGUATT. Goat anti-rabbit-HRP conjugate and goat anti-mouse HRP were purchased from Sigma-Aldrich. Nuclear extraction and DNA binding kits were obtained from Active Motif (Carlsbad, CA, USA). STAT3 and scrambled control siRNAs were obtained from Santa Cruz Biotechnology. Bacteria-derived recombinant human IL-6 was purchased from ProSpec-Tany TechnoGene Ltd. (Rehovot, Israel).

Results

We investigated the effect of emodin on STAT3 activation and on various markers of cellular proliferation, cell survival, and apoptosis in HCC cell lines and an orthotopic mouse model. The structure of emodin is shown in Figure 1A.

Predictive analysis for the effect of emodin on HCC cells

We first tested the potential effect of emodin on the STAT3 activation pathway in the virtual tumour cell system aligned to the human HCC HepG2 cell line. Emodin was observed to have an inhibitory effect on STAT3 activity quite similar to STAT3 inhibition alone by 40% (Figure 1B). JAK2 and SRC kinases also showed an equivalent reduction with both emodin treatment and STAT3 inhibition alone (Figure 1C). This was further confirmed by experimental studies on HepG2 cell line as detailed in the sections below. Reduction in the levels of key genes such as CCND1, cMYC, BCL2, BCL-xl, XIAP and survivin activated downstream of STAT3 was observed with emodin treatment. STAT3 inhibition alone also caused a similar or lesser reduction in these markers (Figure 1C and D), implicating a possible involvement of STAT3 for the emodin-mediated inhibitory effects. An increase in the levels of caspase-3 and cleaved PARP1 was also observed with emodin treatment (Figure 1E).

Emodin inhibits constitutive STAT3 phosphorylation in HepG2 cells

The ability of emodin to modulate constitutive STAT3 activation in HCC cells was investigated by incubating HepG2 cells with different concentrations of emodin for 6 h. Whole cell extracts were prepared and the phosphorylation of STAT3 was examined by Western blot analysis using antibodies which recognize STAT3 phosphorylation at tyrosine 705. As shown in Figure 2A, emodin inhibited the constitutive activation of STAT3 in HepG2 cells in a dose-dependent manner, with maximum inhibition occurring at around 50 μM, but had no effect on the expression of STAT3 protein (Figure 2A; lower panel). We also determined the length of incubation time required for the suppression of STAT3 activation by emodin in HepG2 cells. As shown in Figure 2B, the inhibition was

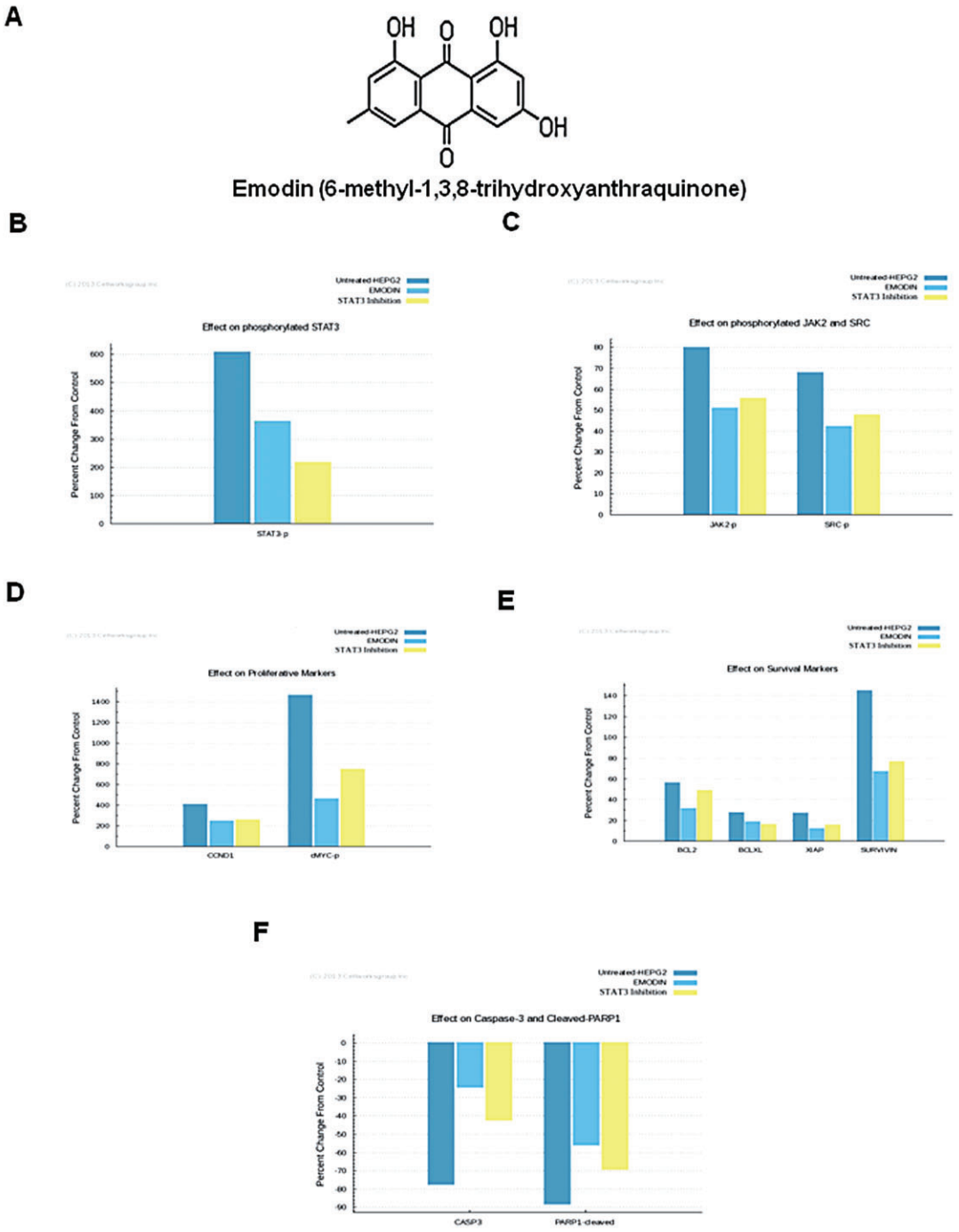

Figure 1

Results generated by predictive proteomics *in silico* using a virtual tumour platform. (A) The chemical structure of emodin. (B) The graph illustrates the percentage reduction in phosphorylated levels of STAT3. STAT3 is showing a reduction of 35% with emodin treatment in the HEPG2 baseline as compared with the untreated placebo. STAT3 activity was also inhibited separately by 40% to compare its effect with emodin treatment. (C) The graph illustrates the percentage reduction in JAK2 and SRC with emodin treatment. The percentage reduction is around 16% for JAK 2 and 15% for SRC with emodin. STAT3 inhibition alone is also showing similar effects on these kinases with the effect being 14% for JAK2 and 12% for SRC. (D) The graph illustrates the percentage change in proliferation markers – CCND1 and cMYC. CCND1 is showing a reduction of 32% from the baseline and the reduction in cMYC is 65% with respect to the untreated baseline. STAT3 inhibition alone is showing a similar reduction of 30% in CCND1 and 50% reduction in cMYC. (E) The graph illustrates the percentage reduction in survival markers with emodin treatment and STAT3 inhibition alone. The percentage reduction is 16% for BCL2, 7% for BCL-xL, 12% for XIAP and 32% for survivin with emodin treatment. The reduction with STAT3 inhibition alone is 5% for Bcl-2, 9% in Bcl-xL, 10% for XIAP and 28% for surviving. (F) The graph illustrates the percentage change in CASP3 and PARP1 cleaved with emodin treatment and STAT3 inhibition alone. An increase of approximately 3.5-fold is seen in the levels of both CASP3 and PARP1 cleaved with emodin treatment. The increase was approximately 2.6-fold with STAT3 inhibition alone.

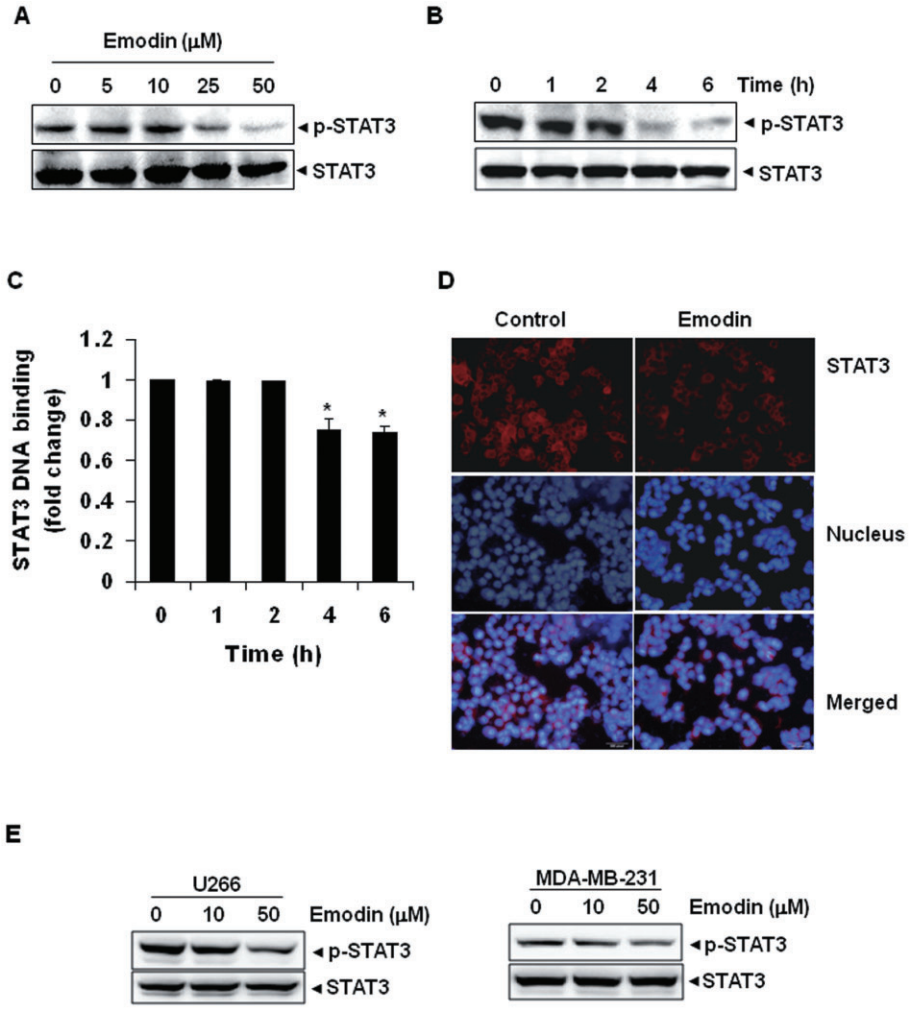

Figure 2

Emodin inhibits constitutively active STAT3 in HepG2 cells. (A) Emodin suppresses phospho-STAT3 levels in a dose-dependent manner. HepG2 cells (2×10^6·mL^{-1}) were treated with the indicated concentrations of emodin for 6 h, after which whole cell extracts were prepared, and 30 μg of protein was resolved on 7.5% SDS-PAGE gel, electrotransferred onto nitrocellulose membranes, and probed for phospho-STAT3/STAT3 proteins. (B) Emodin suppresses phospho-STAT3 levels in a time-dependent manner. HepG2 cells (2×10^6·mL^{-1}) were treated with 50 μM emodin for the indicated times, after which Western blotting was performed as described for panel B. (C) Emodin suppresses STAT3 DNA-binding ability in HepG2 cells. HepG2 cells were treated with 50 μM emodin for indicated time points; nuclear extracts were prepared, and 20 μg of the nuclear extract protein was used for ELISA-based DNA-binding assay. The results shown are representative of two independent experiments. *$P < 0.05$. (D) Emodin causes inhibition of translocation of STAT3 to the nucleus. HepG2 cells (1×10^5·mL^{-1}) were incubated with or without 50 μM emodin for 6 h and then analysed for the intracelullar distribution of STAT3 by immunocytochemistry. The same slides were counterstained for nuclei with Hoechst (50 ng·mL^{-1}) for 5 min. The results shown are representative of three independent experiments. (E) Multiple myeloma (U266) and breast adenocarcinoma (MDA-MB-231) cells (2×10^6·mL^{-1}) were treated with the indicated concentrations of emodin for 6 h, after which whole cell extracts were prepared, and 30 μg of protein was resolved on 7.5% SDS-PAGE gel, electrotransferred onto nitrocellulose membranes, and probed for phospho-STAT3/STAT3 proteins.

time dependent, with substantial inhibition occurring at around 6 h, again with no effect on the expression of STAT3 protein (Figure 2B; lower panel).

Emodin inhibits binding capacity of STAT3 to the DNA

Because tyrosine phosphorylation causes the dimerization of STATs and their translocation to the nucleus, where they bind to DNA and regulate gene transcription (Ihle, 1996; Subramaniam *et al.*, 2013b), we determined whether emodin can modulate the DNA-binding ability of STAT3. Analysis of nuclear extracts prepared from HepG2 cells using ELISA-based TransAM STAT3 assay kit showed that emodin inhibited STAT3-DNA binding activity in a time-dependent manner (Figure 2C).

Emodin reduces nuclear pool of STAT3 in HCC cells

Because the active dimer of STAT3 is capable of translocating to the nucleus and inducing transcription of specific target

genes (Subramaniam *et al.*, 2013b), we next analysed whether emodin can suppress nuclear translocation of STAT3. Figure 2D clearly demonstrates that emodin inhibited the translocation of STAT3 to the nucleus in HepG2 cells.

Inhibitory effects of emodin on STAT3 activation are not cell-type specific

We also investigated whether emodin can modulate constitutively active STAT3 in cells other than HCC. Because multiple myeloma (U266) and breast adenocarcinoma (MDA-MB-231) cells express constitutively active STAT3, we investigated whether emodin could also inhibit STAT3 activation in these cells. Interestingly, emodin was found to suppress STAT3 activation in U266 and MDA-MB-231 cells in a dose-dependent manner, with maximum inhibition occurring at 50 μM after 6 h of treatment (Figure 2E).

Emodin inhibits inducible STAT3 and JAK1/2 phosphorylation in HCC cells

Because IL-6 induces STAT3 phosphorylation (Ihle, 1996), we next determined whether emodin could inhibit IL-6-induced STAT3 phosphorylation in HCC cells. Hence, in HUH-7 cells that display relatively low levels of constitutively active STAT3, IL-6-induced STAT3 and JAK1 phosphorylation was suppressed by emodin in a time-dependent manner. Exposure of cells to emodin for 6 h was sufficient to substantially suppress IL-6-induced STAT3 and JAK1 phosphorylation in HUH-7 cells (Figure 3A and B). Furthermore, we found that emodin can inhibit JAK2 phosphorylation induced by IL-6 in HUH-7 cells (Figure 3C). These results suggest that emodin can also down-regulate inducible STAT3 activation and corroborate with the predictive data on STAT3 inhibition as shown in Figure 1B.

Emodin inhibits IL-6-inducible Akt phosphorylation in HCC cells

Activation of Akt has also been linked with STAT3 activation in tumour cells (Chen *et al.*, 1999). We also next examined whether emodin could modulate IL-6-induced Akt activation. Treatment of HUH-7 cells with IL-6-induced phosphorylation of Akt and the pre-treatment of cells with emodin suppressed the phosphorylation of Akt (Figure 3D). Under these conditions, emodin had no effect on the expression of Akt protein.

Emodin suppresses EGF-induced STAT3-dependent reporter gene expression

Our above results showed that emodin inhibited the phosphorylation and nuclear translocation of STAT3. We next determined whether emodin affects STAT3-dependent gene transcription. When PLC/PRF/5 cells transiently transfected with the pSTAT3-Luc construct were stimulated with EGF, STAT3-mediated luciferase gene expression was increased. Transient transfection with dominant-negative STAT3 blocked this increase, indicating specificity. When the cells were pre-treated with emodin, EGF-induced STAT3 activity was inhibited in a dose-dependent manner (Figure 3E).

Emodin suppresses constitutive activation of c-Src

STAT3 has also been reported to be activated by tyrosine kinases of the Src kinase families (Schreiner *et al.*, 2002). Hence, we determined whether emodin can modulate the constitutive activation of Src kinase in HepG2 cells. We found that emodin suppressed the constitutive phosphorylation of c-Src kinases (Figure 4A). These results confirmed the predictions from the virtual tumour model. The levels of non-phosphorylated Src kinases remained unchanged under the same conditions.

Emodin suppresses constitutive activation of JAK1 and JAK2 in HCC cells

Because STAT3 is also activated by soluble tyrosine kinases of the Janus family (JAKs) (Ihle, 1996), we next analysed whether emodin can affect constitutive activation of JAK1 in HepG2 cells. Emodin suppressed the constitutive phosphorylation of JAK1 (Figure 4B). The levels of non-phosphorylated JAK1 remained unchanged under the same conditions (Figure 4B, bottom panel). To determine the effect of emodin on JAK2 activation, HepG2 cells were treated for different time intervals with emodin and phosphorylation of JAK2 was analysed by Western blot. As shown in Figure 4C, JAK2 was constitutively active in HepG2 cells and pre-treatment with emodin suppressed this phosphorylation in a time-dependent manner.

Tyrosine phosphatases are involved in emodin-induced inhibition of STAT3 activation

Because protein tyrosine phosphatases (PTPs) have also been implicated in STAT3 activation (Han *et al.*, 2006), we determined whether emodin-induced inhibition of STAT3 tyrosine phosphorylation could be due to activation of a PTP (PTPase). Treatment of HepG2 cells with the broad-acting tyrosine phosphatase inhibitor sodium pervanadate reversed emodin-induced suppression of STAT3 activation (Figure 4D). These data suggest that tyrosine phosphatases are involved in emodin-induced inhibition of STAT3 activation.

Emodin induces the expression of SHP-1 in HCC cells

SHP-1 is a non-transmembrane PTP that has been linked with regulation of STAT3 activation (Calvisi *et al.*, 2006). Whether inhibition of STAT3 phosphorylation by emodin is due to induction of the expression of SHP-1 was examined in HepG2 cells. Cells were incubated with emodin for different time intervals; whole-cell extracts were prepared and examined for SHP-1 protein expression by Western blot analysis. As shown in Figure 4E, emodin induced the expression of SHP-1 protein in HepG2 cells in a time-dependent manner, with maximum expression observed after 6 h. This stimulation of SHP-1 expression by emodin correlated with down-regulation of constitutive STAT3 activation in HepG2 cells (Figure 2B). Therefore, these results suggest that stimulation of SHP-1 expression by emodin may mediate the down-regulation of constitutive STAT3 activation in HCC cells.

SHP-1 siRNA down-regulated the expression of SHP-1 induced by emodin

We showed above that the dephosphorylation of STAT3 by emodin correlates with the increased expression of SHP-1. Whether the suppression of SHP-1 expression by siRNA

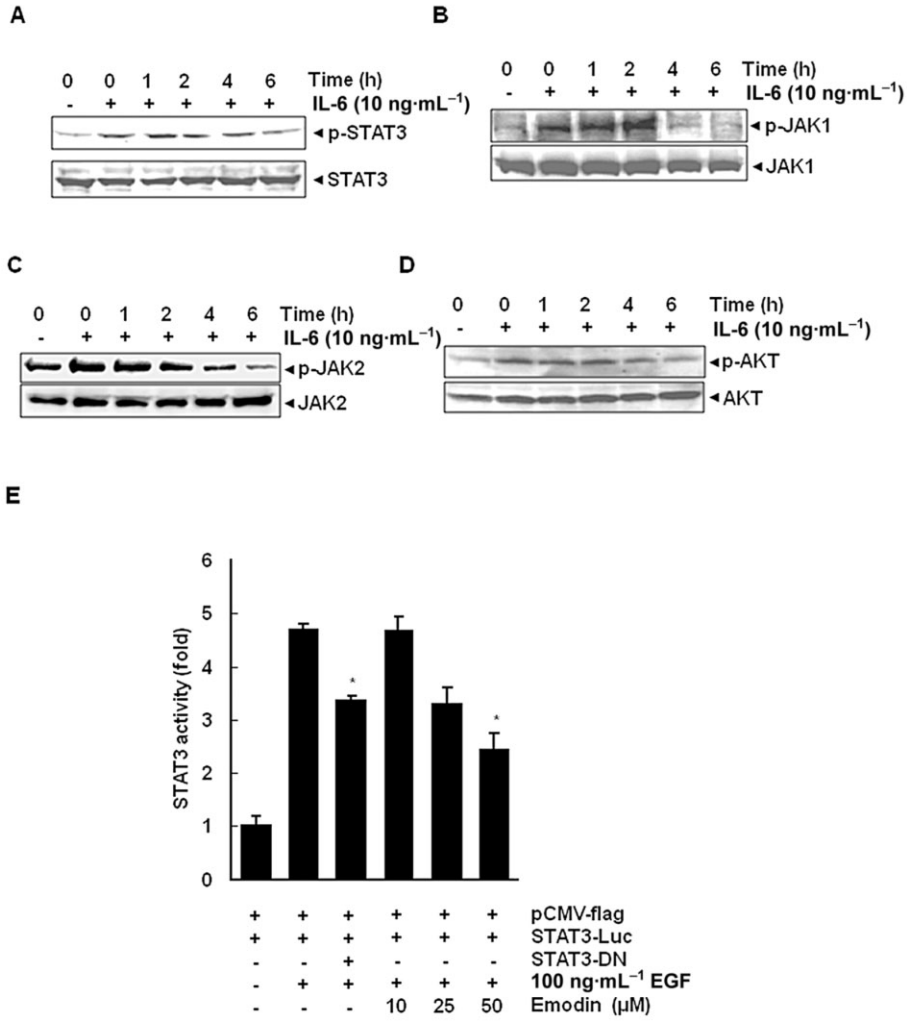

Figure 3

HUH-7 cells ($2 \times 10^6 \cdot mL^{-1}$) were treated with 50 μM emodin for the indicated times and then stimulated with IL-6 (10 $ng \cdot mL^{-1}$) for 15 min. Whole cell extracts were then prepared and analysed for phospho-STAT3/STAT3 by Western blotting. The results shown are representative of three independent experiments. (B) HUH-7 cells ($2 \times 10^6 \cdot mL^{-1}$) were treated with 50 μM emodin for the indicated times and then stimulated with IL-6 (10 $ng \cdot mL^{-1}$) for 15 min. Whole cell extracts were then prepared and analysed for phospho-JAK1/JAK1 by Western blotting. (C) HUH-7 cells ($2 \times 10^6 \cdot mL^{-1}$) were treated with 50 μM emodin for the indicated times and then stimulated with IL-6 (10 $ng \cdot mL^{-1}$) for 15 min. Whole cell extracts were then prepared and analysed for phospho-JAK2/JAK2 proteins. (D) HUH-7 cells ($2 \times 10^6 \cdot mL^{-1}$) were treated with 50 μM emodin for the indicated times and then stimulated with IL-6 (10 $ng \cdot mL^{-1}$) for 15 min. Whole cell extracts were then prepared and analysed for phospho-Akt by Western blotting. The same blots were stripped and reprobed with Akt antibody to verify equal protein loading. (E) PLC/PRF/5 cells ($5 \times 10^5 \cdot mL^{-1}$) were transfected with STAT3-luciferase (STAT3-Luc) plasmid, incubated for 24 h, and treated with 10, 25 and 50 μM emodin for 6 h and then stimulated with EGF (100 $ng \cdot mL^{-1}$) for 2 h. Whole cell extracts were then prepared and analysed for luciferase activity. The results shown are representative of three independent experiments. *$P < 0.05$, significantly different from EGF alone; Student's *t*-test.

would prevent the inhibitory effect of emodin on STAT3 activation was also investigated. As observed by Western blot analysis, emodin-induced SHP-1 expression was effectively inhibited in the cells transfected with SHP-1 siRNA, but not in those treated with the scrambled siRNA (Figure 4F).

SHP-1 siRNA reversed the inhibition of STAT3 activation by emodin

We next determined whether the suppression of SHP-1 expression by siRNA blocked the inhibitory effect of emodin on STAT3 activation. We found that emodin failed to suppress STAT3 activation in the cells transfected with SHP-1 siRNA (Figure 4G). However, in cells transfected with scrambled siRNA, emodin caused down-regulation of STAT3 activation. Thus, these results with siRNA demonstrate the pivotal role of SHP-1 in suppression of STAT3 phosphorylation by emodin.

Emodin down-regulates the expression of cyclin D1, Bcl-2, Bcl-xL, Mcl-1, survivin and VEGF

STAT3 activation has been shown to regulate the expression of various gene products involved in proliferation,

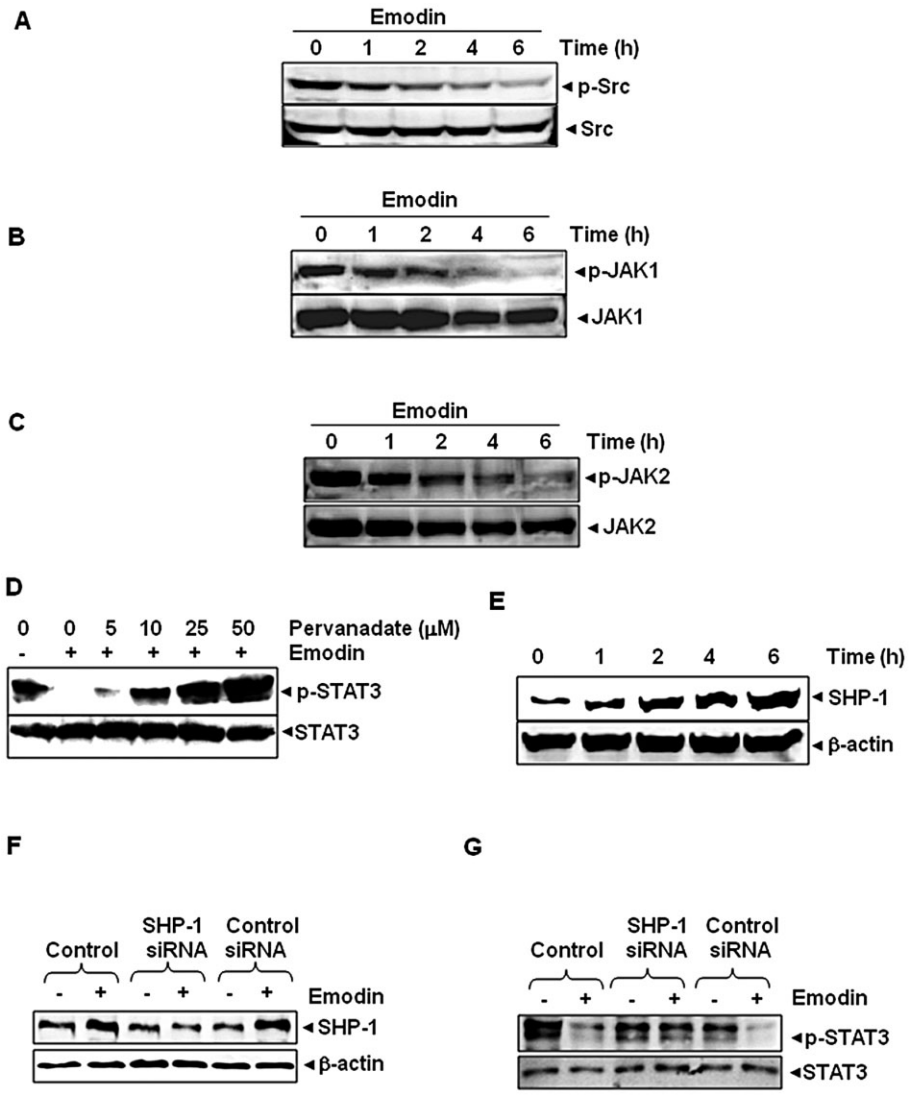

Figure 4

(A) Emodin suppresses phospho-Src levels in a time-dependent manner. HepG2 cells ($2 \times 10^6 \cdot mL^{-1}$) were treated with 50 μM emodin, after which whole cell extracts were prepared and 30 μg of aliquots of those extracts were resolved on 10% SDS-PAGE, electrotransferred onto nitrocellulose membranes, and probed for phospho-Src/Src antibodies. (B) Emodin suppresses phospho-JAK1 levels in a time-dependent manner. HepG2 cells ($2 \times 10^6 \cdot mL^{-1}$) were treated with 50 μM emodin for indicated time intervals, after which whole cell extracts were prepared and 30 μg portions of those extracts were resolved on 10% SDS-PAGE, electrotransferred onto nitrocellulose membranes, and probed with phospho-JAK1/JAK1 antibodies. (C) Emodin suppresses phospho-JAK2 levels in a time-dependent manner. HepG2 cells ($2 \times 10^6 \cdot mL^{-1}$) were treated with 50 μM emodin for indicated time intervals, after which whole cell extracts were prepared and 30 μg portions of those extracts were resolved on 10% SDS-PAGE, electrotransferred onto nitrocellulose membranes, and probed with phospho-JAK2/JAK2 antibodies. (D) Pervanadate reverses the phospho-STAT3 inhibitory effect of emodin. HepG2 cells ($2 \times 10^6 \cdot mL^{-1}$) were treated with the indicated concentrations of pervanadate and 50 μM emodin for 6 h, after which whole cell extracts were prepared and 30 μg portions of those extracts were resolved on 7.5% SDS-PAGE gel, electrotransferred onto nitrocellulose membranes, and probed for phospho-STAT3 and STAT3. (E) Emodin induces the expression of SHP-1 protein in HepG2 cells. HepG2 cells were treated with indicated concentrations of emodin for 6 h, after which Western blotting was performed. (F) Effect of SHP-1 knock-down on emodin-induced expression of SHP-1. HepG2 cells were transfected with either SHP-1 siRNA or scrambled siRNA (50 nM). After 24 h, cells were treated with 50 μM emodin for 6 h and whole cell extracts were subjected to Western blot analysis. (G) HepG2 cells were transfected with either SHP-1 siRNA or scrambled siRNA (50 nM). After 24 h, cells were treated with 50 μM emodin for 6 h and whole cell extracts were subjected to Western blot analysis for phosphorylated STAT3. The results shown are representative of three independent experiments.

anti-apoptosis, invasion, angiogenesis and chemoresistance (Johnston and Grandis, 2011). Expression of the cell cycle regulator cyclin D1, the anti-apoptotic proteins Bcl-2, survivin, Mcl-1 and the angiogenic gene product VEGF all of which have been reported to be regulated by STAT3 were modulated by emodin treatment in HepG2 cells. Their expression decreased in a time-dependent manner, with maximum suppression observed at around 24 h (Figure 5A).

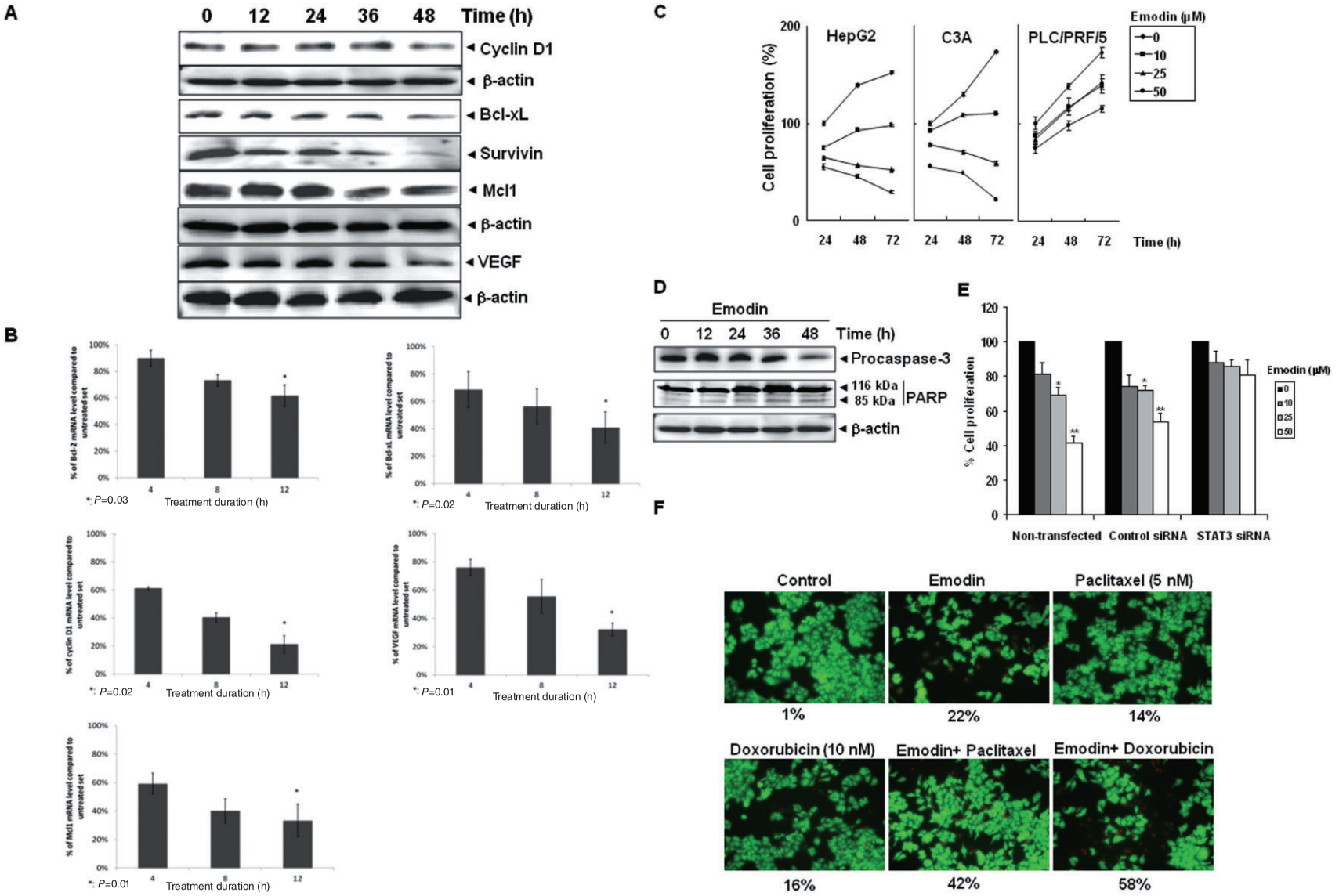
A
0 12 24 36 48 Time (h)
Cyclin D1
β-actin
Bcl-xL
Survivin
Mcl1
β-actin
VEGF
β-actin
B
% of Bcl-2 mRNA level compared to untreated set
*: P=0.03
Treatment duration (h)
% of Bcl-xL mRNA level compared to untreated set
*: P=0.02
Treatment duration (h)
% of cyclin D1 mRNA level compared to untreated set
*: P=0.02
Treatment duration (h)
% of VEGF mRNA level compared to untreated set
*: P=0.01
Treatment duration (h)
% of Mcl1 mRNA level compared to untreated set
*: P=0.01
Treatment duration (h)
C
Cell proliferation (%)
HepG2
C3A
PLC/PRF/5
Emodin (μM)
0
10
25
50
24 48 72 24 48 72 24 48 72 Time (h)
D
Emodin
0 12 24 36 48 Time (h)
Procaspase-3
116 kDa
85 kDa
PARP
β-actin
E
% Cell proliferation
Emodin (μM)
0
10
25
50
Non-transfected
Control siRNA
STAT3 siRNA
F
Control
Emodin
Paclitaxel (5 nM)
1%
22%
14%
Doxorubicin (10 nM)
Emodin+ Paclitaxel
Emodin+ Doxorubicin
16%
42%
58%

We also found that mRNA expression of Bcl-2, Bcl-xL, survivin, Mcl-1 and VEGF was modulated by emodin treatment in a time-dependent manner with maximum reduction observed at around 12 h after treatment (Figure 5B). These results also support the predictive analysis seen with STAT3 inhibition on these markers as seen in Figure 1C and D.

Emodin inhibits the proliferation of HCC cells in a dose- and time-dependent manner

Because emodin down-regulated the expression of cyclin D1, a gene involved in cell proliferation, we investigated whether emodin inhibits the proliferation of HCC cells by using the MTT assay. Emodin inhibited the proliferation of HepG2 and C3A cells in a dose- and time-dependent manner, whereas it had relatively little effect on the proliferation of PLC/PRF/5 cells (Figure 5C).

Emodin activates caspase-3 and causes PARP cleavage

Whether suppression of constitutively active STAT3 in HepG2 cells by emodin leads to apoptosis was also investigated. In HepG2 cells treated with emodin, there was a time-dependent activation of pro-caspase-3 (Figure 5D). Activation of downstream caspases led to the cleavage of a 118 kDa PARP protein into an 85 kDa fragment (Figure 5D). These results clearly suggest that emodin induces caspase-3-dependent apoptosis in HepG2 cells.

Transfection with STAT3 siRNA blocks the anti-proliferative effects of emodin in HCC cells

We determined whether the suppression of STAT3 expression by siRNA could blockthe anti-proliferative effect of emodin on HCC cells. Results shown in Figure 5E clearly indicate that the observed anti-proliferative effect of emodin was significantly abolished in the cells transfected with STAT3 siRNA, whereas treatment with control siRNA had minimal effect (Figure 5E). These results suggest that inhibition of proliferation is mediated at least in part through the suppression of STAT3 in HCC cells by emodin.

Emodin potentiates the apoptotic effect of doxorubicin and paclitaxel in HepG2 cells

Among chemotherapeutic agents, doxorubicin, an anthracycline antibiotic, and paclitaxel, a mitotic inhibitor, have been used for HCC treatment (Cervello *et al.*, 2012; Subramaniam *et al.*, 2013b). We examined whether emodin can potentiate the effect of these drugs. HepG2 cells were treated with emodin together with either doxorubicin or paclitaxel, and then apoptosis was measured by the live/dead assay. As shown in Figure 5F, emodin substantially enhanced the apoptotic effects of doxorubicin and of paclitaxel.

Emodin suppresses the growth of human HCC in vivo *and STAT3 activation in tumour tissues*

We tested the anti-tumour potential of emodin *in vivo* via i.p. administration in an orthotopic model of human HCC using HCCLM3_Luc2 tumour stably expressing firefly luciferase.

Figure 5

Emodin suppresses STAT3-regulated gene products involved in proliferation, survival and angiogenesis. (A) HepG2 cells (2×10^6·mL^{-1}) were treated with 50 μM emodin for indicated time intervals, after which whole cell extracts were prepared and 30 μg portions of those extracts were resolved on 10% SDS-PAGE, membrane sliced according to molecular weight and probed against cyclin D1, Bcl-2, survivin, Mcl-1 and VEGF antibodies. The same blots were stripped and reprobed with β-actin antibody to verify equal protein loading. The results shown are representative of three independent experiments. (B) HepG2 cells (3×10^5·mL^{-1}) were treated with 50 μM emodin for the indicated time intervals, after which cells were harvested after treatment and RNA samples were extracted. About 1 μg portions of the respective RNA extracts were used for reverse transcription to generate corresponding cDNA. Real-time PCR was performed to measure the relative quantities of mRNA. Each RT product was targeted against cyclin D1, Bcl-2, Bcl-X_L, Mcl-1 and VEGF TaqMan probes, with HuGAPDH as endogenous control for measurement of equal loading of RNA samples. Results were analysed using Sequence Detection Software version 1.3 provided by Applied Biosystems (Foster City, CA, USA). Relative gene expression was obtained after normalization with endogenous HuGAPDH and determination of the difference in threshold cycle (Ct) between treated and untreated cells using 2-ΔΔCt method. (C) HepG2, C3A and PLC/PRF/5 cells (5×10^3·mL^{-1}) were plated in triplicate, treated with indicated concentrations of emodin, and then subjected to MTT assay after 24, 48 and 72 h to measure the proliferation of cells. SDs between the triplicates are indicated. (D) HepG2 cells were treated with 50 μM emodin for the indicated times, whole cell extracts were prepared, separated on SDS-PAGE, and subjected to Western blotting against pro-caspase-3 and PARP antibodies. The same blot was stripped and reprobed with β-actin antibody to show equal protein loading. The results shown are representative of three independent experiments. (E) Knock-down of STAT3 siRNA reduces the anti-proliferative effect of emodin. HepG2 cells were transfected with either STAT3-specific or control siRNA (50 nM). After 48 h, cells were treated with indicated concentrations of emodin for 72 h and then subjected to MTT assay, *$P \leq 0.05$; **$P \leq 0.005$, significant effect of emodin; Student's *t*-test. (F) Emodin potentiates the apoptotic effect of doxorubicin and paclitaxel. HepG2 cells (1×10^6·mL^{-1}) were treated with 10 μM emodin and 10 nM doxorubicin or 5 nM paclitaxel alone or in combination for 24 h at 37°C. Cells were stained with a live/dead assay reagent for 30 min and then the percentage of apoptotic cells was determined , using a fluorescence microscope.

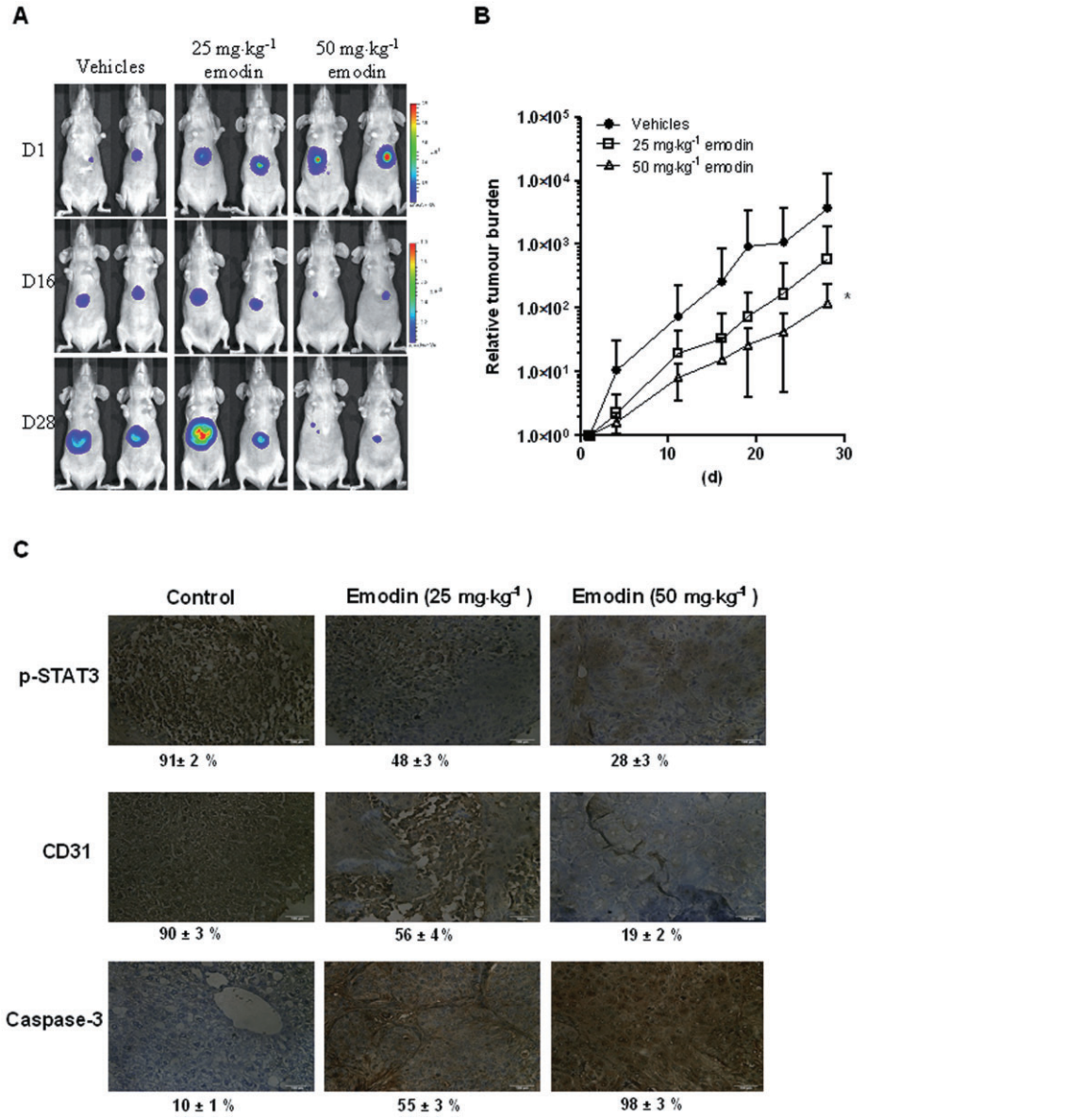

Figure 6

Emodin inhibits the growth of human HCC *in vivo*. (A) Representative images of mice from bioluminescent imaging. D = day. (B) Relative tumour burden in athymic mice bearing orthotopically implanted HCCLM3-Luc2 tumours treated with vehicle alone (n = 9), 25 mg·kg^{-1} (n = 10) or 50 mg·kg^{-1} (n = 9) of emodin. Points, mean; bars, SE. * P < 0.05, significant effect of emodin; one-way ANOVA. (C) Immunohistochemical analysis of p-STAT3, CD31 and caspase-3 showed the inhibition in expression of p-STAT3, and CD31 and increased levels of caspase-3 expression in emodin-treated samples as compared with control group. Percentage indicates positive staining for the biomarker shown. The photographs were taken at magnification 40×.

Orthotopic tumour growth was monitored non-invasively using bioluminescence imaging. Prior to the first therapeutic injection (10 d after tumour implantation), growing orthotopic tumours were detected using bioluminescence imaging and found to localize mainly at the liver (Figure 6A). Mice were treated with five doses a week of either vehicle alone (n = 9), 25 mg·kg^{-1} (n = 10) or 50 mg·kg^{-1} (n = 9) of emodin for up to 3 weeks. Bioluminescence images revealed that there was significant inhibition of tumour growth in the 50 mg·kg^{-1} emodin-treated group compared with the vehicle control group (Figure 6A). Differences in tumour burden at set time points were quantitated by measuring photon counts and expressed as tumour burden relative to photon counts before first therapeutic injection (Figure 6B). One-way ANOVA indicated that emodin at 50 mg·kg^{-1} induced significant inhibition of tumour growth compared with the vehicle-treated controls (Figure 6B). We further evaluated the effect of emodin on constitutive p-STAT3 levels in HCC tumour tissues by immunohistochemical analysis and found that emodin substantially inhibited the constitutive STAT3 activation in

treated group as compared with control group (Figure 6C). The effect of emodin was also analysed on the expression of CD31 (marker of angiogenesis) and caspase-3 (marker of apoptosis). As shown in Figure 6C, expression of CD31 was down-regulated and that of caspase-3 was substantially increased in emodin-treated group as compared with control group.

Discussion

The main aim of this study was to determine whether emodin exerts its anti-cancer effects through the blockade of the STAT3 signalling pathway in HCC cells. We found that emodin suppressed constitutive and inducible STAT3 activation in human HCC cells in parallel with the inhibition of c-Src, JAK1 and JAK2 activation. Emodin also down-regulated the expression of STAT3-regulated gene products including cyclin D1, Bcl-2, Bcl-xL, survivin, Mcl-1 and VEGF. It also caused the inhibition of proliferation and induced substantial apoptosis in HCC cells. We further investigated the potential therapeutic efficacy of emodin in an *in vivo* model of HCC in mice. Intraperitoneal injection of emodin in an orthotopic model of human HCC resulted in a significant suppression of tumour progression and suppression of expression of p-STAT3 in emodin-treated tumour tissues. This hypothesis was also tested in a virtual predictive tumour cell system and orthotopic mice model and the experimental results clearly indicate that emodin mediates its suppressive effects on the STAT3 activation cascade in HCC.

This is the first report to systematically analyse the potential effects of emodin on STAT3 activation in HCC cells and an orthotopic mice model. Whether examined by STAT3 phosphorylation at tyrosine 705, by nuclear translocation and by DNA binding, we found that emodin suppressed STAT3 activation. This was also shown in the virtual predictive analysis where the inhibitory effects of emodin were observed to be similar to the effect of inhibition of STAT3 activity alone. The reduction in survival markers like Bcl-2, Bcl-xL, XIAP and survivin was similar for HepG2 cells treated with emodin and STAT3 inhibition alone, emphasizing that emodin may have its downstream effects via inhibition of STAT3 activity. Emodin also suppressed STAT3 activation induced by IL-6, one of the many tumour cell growth factors that activate STAT3 (Bromberg and Wang, 2009). The doses required to inhibit STAT3 activation were very comparable to rationally designed chemical inhibitors that inhibit STAT3 dimerization (Fuke *et al.*, 2007).

How emodin inhibits activation of STAT3 was also investigated in detail. The activation of JAK has been closely linked with STAT3 activation (Ihle, 1996) and we observed that emodin inhibited the activation of constitutively active JAK1 and JAK2 in HCC cells. This is in agreement with a report that AZD1480, a pharmacological JAK2 inhibitor, can significantly suppress STAT3 signalling and oncogenesis (Hedvat *et al.*, 2009). We further found that the IL-6-induced STAT3 and JAK1/2 activation was also suppressed by emodin. Our results are partially in agreement with a previous report by Muto and co-workers who observed that emodin indeed can suppress STAT3/JAK2 signalling cascade in multiple myeloma cells (Muto *et al.*, 2007), but they did not investigate the detailed molecular mechanisms of their observations. Overall, we noticed that emodin could indeed suppress both constitutive and inducible STAT3 activation in HCC cells leading to the other downstream effects as confirmed through the corroboration between the experimental and predictive data.

We also found evidence that the emodin-induced inhibition of STAT3 activation involves a PTP. Numerous PTPs have been implicated in STAT3 signalling including SHP-1, SH-PTP2, TC-PTP, PTEN, PTP-1D, CD45, PTP-ε, low molecular weight and PTP (Tan *et al.*, 2010). SHP-1 is implicated in negative regulation of JAK/STAT signalling pathways and it has been found that loss of SHP-1 may contribute to the activation of JAK or STAT proteins in cancer (Wu *et al.*, 2003). Indeed, we found for the first time that emodin induces the expression of SHP-1 protein in HCC cells, which correlated, with down-regulation of constitutive STAT3 phosphorylation. Transfection with SHP-1 siRNA reversed the STAT3 inhibitory effect of emodin, thereby further implicating a crucial role of this phosphatase in emodin-induced down-regulation of STAT3 activation. Also, it has been reported previously that emodin can also suppress NF-κB activation in various cell lines and mouse models of inflammation and cancer (Meng *et al.*, 2010; Liu *et al.*, 2011). Whether suppression of STAT3 activation by emodin can also be linked to inhibition of NF-κB activation is not clear as yet, although an earlier study had indicated that STAT3 can prolong NF-κB nuclear retention through acetyltransferase p300-mediated p65 acetylation, thus interfering with NF-κB nuclear export (Lee *et al.*, 2009). Thus, it is possible that suppression of STAT3 activation may mediate inhibition of NF-κB activation by emodin.

We further found that emodin suppressed the expression of several STAT3-regulated genes, including proliferative (cyclin D1) and anti-apoptotic gene products (Bcl-2, Bcl-xL, survivin and Mcl-1) and angiogenic gene product (VEGF). The down-regulation of cyclin D1 expression correlated with suppression in proliferation as observed in various HCC cell lines and also in agreement with a recent study in human tongue squamous cancer SCC-4 cells where emodin was found to modulate Cdc-2 and cyclin-B1 expression (Lin *et al.*, 2009). Moreover, anti-apoptotic protein Mcl-1 is highly expressed in tumour cells (Epling-Burnette *et al.*, 2001), and the inhibition of STAT3 by a Src inhibitor can lead to down-regulation of expression of *Mcl-1* gene (Niu *et al.*, 2002). In addition, activation of STAT3 signalling induces *survivin* gene expression and confers resistance to apoptosis in breast cancer cells (Gritsko *et al.*, 2006). Bcl-2 and Bcl-xL can also block cell death induced by a variety of chemotherapeutic drugs, and thus contribute to chemoresistance (Seitz *et al.*, 2010). Thus, the down-regulation of the expression of Bcl-2, Bcl-xL, survivin and Mcl-1 is likely to be linked with emodin's ability to induce apoptosis in HCC cells, as documented previously. The downmodulation of VEGF and CD31 expression by emodin as we showed also emphasized the anti-angiogenic potential of emodin in HCC, an aspect which requires further detailed investigation. We also noticed that emodin substantially potentiated the apoptotic effect of doxorubicin and paclitaxel in HCC cells and hence could also be used in conjunction with existing anti-HCC therapies. Additionally, we observed that knocking down the expression of STAT3 by siRNA significantly reduced the anti-proliferative

effect of emodin on HCC cells, thereby supporting our hypothesis that anti-proliferative/pro-apoptotic effects of emodin were mediated at least in part through the abrogation of the STAT3 signalling pathway.

We also observed that emodin significantly suppressed HCC growth in an orthotopic mice model down-regulated the expression of phospho-STAT3 and CD31 and increased the levels of caspase-3 in treated group as compared with control. Moreover, to the best of our knowledge, no prior studies with emodin have been reported in HCC mouse models, and our observations clearly indicate that emodin has a clear potential for the treatment of HCC through the suppression of the STAT3 signalling cascade. These findings are consistent with earlier reports in which emodin has been shown to be well tolerated in preclinical studies, with no reported toxicity (Xu and Lin, 2008; Xia *et al.*, 2009; Meng *et al.*, 2010; Liu *et al.*, 2011). Thus, overall, our *in vitro* and *in vivo* experimental findings substantiated by our predictive analysis clearly indicate that the anti-cancer effects of emodin in HCC are mediated through the suppression of the STAT3 signalling cascade and provide a strong rationale for pursuing the use of emodin to enhance treatment efficacy in HCC patients.

Acknowledgements

This research work was supported by grant from Singapore Ministry of Health's National Medical Research Council under its Exploratory/Developmental Grant (EDG) funding scheme to G. S. K. M. H. was supported by a grant from the National Medical Research Council of Singapore, Biomedical Research Council of Singapore, and the Singapore Millennium Foundation. A. P. K. was supported by grants from Singapore Ministry of Education Tier 2 (MOE2012-T2-2-139), Academic Research Fund Tier 1 (R-184-000-228-112) and Cancer Science Institute of Singapore, Experimental Therapeutics I Program (Grant R-713-001-011-271).

Conflict of interest

None.

References

Alexander SPH, Mathie A, Peters JA (2011). Guide to Receptors and Channels (GRAC), 5th edition. Br J Pharmacol 164 (Suppl. 1): S1–324.

Battistutta R, Sarno S, De Moliner E, Papinutto E, Zanotti G, Pinna LA (2000). The replacement of ATP by the competitive inhibitor emodin induces conformational modifications in the catalytic site of protein kinase CK2. J Biol Chem 275: 29618–29622.

Bromberg J, Wang TC (2009). Inflammation and cancer: IL-6 and STAT3 complete the link. Cancer Cell 15: 79–80.

Brown M, Bellon M, Nicot C (2007). Emodin and DHA potently increase arsenic trioxide interferon-alpha-induced cell death of HTLV-I-transformed cells by generation of reactive oxygen species and inhibition of Akt and AP-1. Blood 109: 1653–1659.

Calvisi DF, Ladu S, Gorden A, Farina M, Conner EA, Lee JS *et al.* (2006). Ubiquitous activation of Ras and Jak/Stat pathways in human HCC. Gastroenterology 130: 1117–1128.

Cervello M, McCubrey JA, Cusimano A, Lampiasi N, Azzolina A, Montalto G (2012). Targeted therapy for hepatocellular carcinoma: novel agents on the horizon. Oncotarget 3: 236–260.

Chen RH, Chang MC, Su YH, Tsai YT, Kuo ML (1999). Interleukin-6 inhibits transforming growth factor-beta-induced apoptosis through the phosphatidylinositol 3-kinase/Akt and signal transducers and activators of transcription 3 pathways. J Biol Chem 274: 23013–23019.

Chen YC, Shen SC, Lee WR, Hsu FL, Lin HY, Ko CH *et al.* (2002). Emodin induces apoptosis in human promyeloleukemic HL-60 cells accompanied by activation of caspase 3 cascade but independent of reactive oxygen species production. Biochem Pharmacol 64: 1713–1724.

Epling-Burnette PK, Liu JH, Catlett-Falcone R, Turkson J, Oshiro M, Kothapalli R *et al.* (2001). Inhibition of STAT3 signaling leads to apoptosis of leukemic large granular lymphocytes and decreased Mcl-1 expression. J Clin Invest 107: 351–362.

Ferlay J, Shin HR, Bray F, Forman D, Mathers C, Parkin DM (2010). Estimates of worldwide burden of cancer in 2008: GLOBOCAN 2008. Int J Cancer 127: 2893–2917.

Fuke H, Shiraki K, Sugimoto K, Tanaka J, Beppu T, Yoneda K *et al.* (2007). Jak inhibitor induces S phase cell-cycle arrest and augments TRAIL-induced apoptosis in human hepatocellular carcinoma cells. Biochem Biophys Res Commun 363: 738–744.

Gritsko T, Williams A, Turkson J, Kaneko S, Bowman T, Huang M *et al.* (2006). Persistent activation of stat3 signaling induces survivin gene expression and confers resistance to apoptosis in human breast cancer cells. Clin Cancer Res 12: 11–19.

Grivennikov SI, Karin M (2010). Dangerous liaisons: STAT3 and NF-kappaB collaboration and crosstalk in cancer. Cytokine Growth Factor Rev 21: 11–19.

Han Y, Amin H, Franko B, Frantz C, Shi X, Lai R (2006). Loss of SHP1 enhances JAK3/STAT3 signaling and decreases proteosome degradation of JAK3 and NPM-ALK in ALK-positive anaplastic large-cell lymphoma. Blood 108: 2796–2803.

Hedvat M, Huszar D, Herrmann A, Gozgit JM, Schroeder A, Sheehy A *et al.* (2009). The JAK2 inhibitor AZD1480 potently blocks Stat3 signaling and oncogenesis in solid tumors. Cancer Cell 16: 487–497.

Huang Q, Shen HM, Ong CN (2004). Inhibitory effect of emodin on tumor invasion through suppression of activator protein-1 and nuclear factor-kappaB. Biochem Pharmacol 68: 361–371.

Ihle JN (1996). STATs: signal transducers and activators of transcription. Cell 84: 331–334.

Johnston PA, Grandis JR (2011). STAT3 signaling: anticancer strategies and challenges. Mol Interv 11: 18–26.

Kilkenny C, Browne W, Cuthill IC, Emerson M, Altman DG (2010). Animal research: Reporting *in vivo* experiments: The ARRIVE guidelines. Br J Pharmacol 160: 1577–1579.

Lee H, Herrmann A, Deng JH, Kujawski M, Niu G, Li Z *et al.* (2009). Persistently activated Stat3 maintains constitutive NF-kappaB activity in tumors. Cancer Cell 15: 283–293.

Lin H, van den Esschert J, Liu C, van Gulik TM (2011). Systematic review of hepatocellular adenoma in China and other regions. J Gastroenterol Hepatol 26: 28–35.

Lin SY, Lai WW, Ho CC, Yu FS, Chen GW, Yang JS *et al.* (2009). Emodin induces apoptosis of human tongue squamous cancer SCC-4 cells through reactive oxygen species and mitochondria-dependent pathways. Anticancer Res 29: 327–335.

Liu A, Chen H, Tong H, Ye S, Qiu M, Wang Z *et al.* (2011). Emodin potentiates the antitumor effects of gemcitabine in pancreatic cancer cells via inhibition of nuclear factor-kappaB. Mol Med Rep 4: 221–227.

Manu KA, Shanmugam MK, Ong TH, Subramaniam A, Siveen KS, Perumal E *et al.* (2013). Emodin suppresses migration and invasion through the modulation of CXCR4 expression in an orthotopic model of human hepatocellular carcinoma. PLoS ONE 8: e57015.

McGrath J, Drummond G, Kilkenny C, Wainwright C (2010). Guidelines for reporting experiments involving animals: the ARRIVE guidelines. Br J Pharmacol 160: 1573–1576.

Meng G, Liu Y, Lou C, Yang H (2010). Emodin suppresses lipopolysaccharide-induced pro-inflammatory responses and NF-kappaB activation by disrupting lipid rafts in CD14-negative endothelial cells. Br J Pharmacol 161: 1628–1644.

Muto A, Hori M, Sasaki Y, Saitoh A, Yasuda I, Maekawa T *et al.* (2007). Emodin has a cytotoxic activity against human multiple myeloma as a Janus-activated kinase 2 inhibitor. Mol Cancer Ther 6: 987–994.

Newman DJ (2008). Natural products as leads to potential drugs: an old process or the new hope for drug discovery? J Med Chem 51: 2589–2599.

Niu G, Wright KL, Huang M, Song L, Haura E, Turkson J *et al.* (2002). Constitutive Stat3 activity up-regulates VEGF expression and tumor angiogenesis. Oncogene 21: 2000–2008.

Rajendran P, Ong TH, Chen L, Li F, Shanmugam MK, Vali S *et al.* (2011). Suppression of signal transducer and activator of transcription 3 activation by butein inhibits growth of human hepatocellular carcinoma in vivo. Clin Cancer Res 17: 1425–1439.

Rajendran P, Li F, Shanmugam MK, Kannaiyan R, Goh JN, Wong KF *et al.* (2012). Celastrol suppresses growth and induces apoptosis of human hepatocellular carcinoma through the modulation of STAT3/JAK2 signaling cascade in vitro and in vivo. Cancer Prev Res (Phila) 5: 631–643.

Roy KR, Reddy GV, Maitreyi L, Agarwal S, Achari C, Vali S *et al.* (2010). Celecoxib inhibits MDR1 expression through COX-2-dependent mechanism in human hepatocellular carcinoma (HepG2) cell line. Cancer Chemother Pharmacol 65: 903–911.

Schreiner SJ, Schiavone AP, Smithgall TE (2002). Activation of STAT3 by the Src family kinase Hck requires a functional SH3 domain. J Biol Chem 277: 45680–45687.

Seitz SJ, Schleithoff ES, Koch A, Schuster A, Teufel A, Staib F *et al.* (2010). Chemotherapy-induced apoptosis in hepatocellular carcinoma involves the p53 family and is mediated via the extrinsic and the intrinsic pathway. Int J Cancer 126: 2049–2066.

Shieh DE, Chen YY, Yen MH, Chiang LC, Lin CC (2004). Emodin-induced apoptosis through p53-dependent pathway in human hepatoma cells. Life Sci 74: 2279–2290.

Subramaniam A, Loo SY, Rajendran P, Manu KA, Perumal E, Li F *et al.* (2013a). An anthraquinone derivative, emodin sensitizes hepatocellular carcinoma cells to TRAIL induced apoptosis through the induction of death receptors and downregulation of cell survival proteins. Apoptosis. (in press).

Subramaniam A, Shanmugam MK, Perumal E, Li F, Nachiyappan A, Dai X *et al.* (2013b). Potential role of signal transducer and activator of transcription (STAT)3 signaling pathway in inflammation, survival, proliferation and invasion of hepatocellular carcinoma. Biochim Biophys Acta 1835: 46–60.

Tabolacci C, Lentini A, Mattioli P, Provenzano B, Oliverio S, Carlomosti F *et al.* (2010). Antitumor properties of aloe-emodin and induction of transglutaminase 2 activity in B16-F10 melanoma cells. Life Sci 87: 316–324.

Tan SM, Li F, Rajendran P, Kumar AP, Hui KM, Sethi G (2010). Identification of beta-escin as a novel inhibitor of signal transducer and activator of transcription 3/Janus-activated kinase 2 signaling pathway that suppresses proliferation and induces apoptosis in human hepatocellular carcinoma cells. J Pharmacol Exp Ther 334: 285–293.

Wang H, Lafdil F, Kong X, Gao B (2011). Signal transducer and activator of transcription 3 in liver diseases: a novel therapeutic target. Int J Biol Sci 7: 536–550.

Wang R, Wan Q, Zhang Y, Huang F, Yu K, Xu D *et al.* (2007). Emodin suppresses interleukin-1beta induced mesangial cells proliferation and extracellular matrix production via inhibiting P38 MAPK. Life Sci 80: 2481–2488.

Wang SC, Zhang L, Hortobagyi GN, Hung MC (2001). Targeting HER2: recent developments and future directions for breast cancer patients. Semin Oncol 28 (6 Suppl. 18): 21–29.

Wu C, Guan Q, Wang Y, Zhao ZJ, Zhou GW (2003). SHP-1 suppresses cancer cell growth by promoting degradation of JAK kinases. J Cell Biochem 90: 1026–1037.

Xia QS, Sun RY, Xiu RJ (2009). [Progress of research on molecular mechanisms in antitumor effect of emodin]. Zhongguo Zhong Xi Yi Jie He Za Zhi 29: 85–88.

Xu XC, Lin SZ (2008). [Experimental advance of applying emodin for prevention and treatment of liver diseases]. Zhongguo Zhong Xi Yi Jie He Za Zhi 28: 91–93.